Автономная некоммерческая организация высшего образования «Университет Иннополис»

ВЫПУСКНАЯ КВАЛИФИКАЦИОННАЯ РАБОТА (БАКАЛАВРСКАЯ РАБОТА) по направлению подготовки 09.03.01 - «Информатика и вычислительная техника»

GRADUATION THESIS (BACHELOR'S GRADUATION THESIS) Field of Study 09.03.01 – «Computer Science»

Направленность (профиль) образовательной программы «Информатика и вычислительная техника» Area of Specialization / Academic Program Title: «Computer Science»

Тема / Topic	**Улучшенное управление робототехническими системами в скользящих режимах на основе выпуклой оптимизации / Enhanced Convex Optimization Driven Sliding Mode Control over Robotic Systems**

Работу выполнил / Thesis is executed by	**Ярыева Динара Рифхатовна / Dinara Yaryeva**	подпись / signature
Руководитель выпускной квалификационной работы / Supervisor of Graduation Thesis	**Неделчев Симеон Иванов / Simeon Nedelchev**	подпись / signature

Иннополис, Innopolis, 2024

Contents

List of Tables

List of Figures

Abstract

Controlling Remotely Operated Vehicles (ROVs) in underwater environments is challenging due to their nonlinear and unpredictable nature. This thesis explores enhancing sliding mode control (SMC) for ROVs using convex optimization to improve stability and performance while reducing chattering. A comprehensive mathematical model of an ROV is developed, addressing dynamic and kinematic properties along with environmental uncertainties. An optimized SMC scheme is designed, integrating convex optimization to adjust control parameters dynamically, thus minimizing chattering and enhancing robustness. Validation through simulations and experiments demonstrates significant improvements in trajectory tracking and disturbance rejection. The enhanced SMC scheme proves effective in simulation, confirming its practical applicability. This research advances underwater robotics by providing a robust control strategy that enhances ROV stability and efficiency, supporting complex underwater missions like pipeline inspection and environmental monitoring.

Chapter 1

Introduction

I   Background

Underwater robotic systems, such as Remotely Operated Vehicles (ROVs), have gained significant attention for their diverse applications in industry, science, and the military. ROVs are employed for diverse purposes, including underwater exploration, pipeline inspection, and environmental monitoring. However, controlling these vehicles is challenging due to the highly nonlinear and unpredictable nature of the underwater environment. Therefore, effective control strategies are essential to ensure the stability and performance of ROVs in such conditions.

Control strategies for ROVs have evolved, with robust control methods like Sliding Mode Control (SMC) gaining prominence due to their effectiveness in handling system nonlinearities and uncertainties. Despite these advancements, existing control methods for ROVs face several challenges. Traditional SMC techniques, while robust, often lead to a phenomenon known as "chattering," which can cause wear and tear on mechanical components and reduce the overall efficiency of the control system. Additionally, many control algorithms struggle

to adapt to real-time changes in the underwater environment, such as varying current strengths and unforeseen obstacles. These limitations underscore the need for improved control strategies that can offer both robustness and adaptability.

II   Research Objective

The primary objective of this study is to enhance the control of remotely operated vehicles (ROVs) by developing an improved Sliding Mode Control (SMC) scheme that leverages convex optimization techniques. This thesis aims to address the existing issues of chattering and adaptability by dynamically adjusting control parameters through convex optimization.

The research question: How can sliding mode control for robotic systems be improved using convex optimization to enhance stability and performance while mitigating the chattering effect?

The research objectives are as follows:

1. Develop a comprehensive mathematical model for ROVs that captures the essential dynamics and uncertainties;

2. Design a sliding mode control scheme enhanced by convex optimization;

3. Evaluate the performance of the proposed control scheme through simulation;

III   Structure of the Thesis

The thesis is organized into several chapters to systematically address the research objectives and methodologies. Chapter 1 provides an introduction, out-

lining the background, research objective, and the structure of the thesis. Chapter 2 reviews the existing literature on remotely operated vehicles (ROVs), focusing on modeling and control design. Chapter 3 delves into the mathematical modeling of ROVs, covering the notations, frames of reference, kinematics, dynamics, and thruster modeling. Chapter 4 discusses the methodology, including design considerations, control objectives, model uncertainties, and the approximated system dynamics. Chapter 5 presents the implementation of the proposed control scheme and its validation through simulations and experiments. Finally, Chapter 6 concludes the thesis with a summary of findings, contributions, and suggestions for future research.

Chapter 2

Literature Review

This chapter presents a comprehensive overview of existing research on remotely operated vehicles (ROVs), focusing on modeling and control design. This literature review aims to investigate and synthesize control strategies, addressing uncertainties from actuator dynamics and environmental factors, which correspond to the proposed research question.

Section 1 gives a brief description of ROVs, including their types and general attributes. Section 2 explains the commonly accepted assumptions and mathematical models used in the field. Section 3 offers an extensive review of various studies on the application of robust control design for underwater systems. In conclusion, Section 4 summarizes the key insights from the review and suggests a control methodology.

I Overview on ROVs

This section provides an overview of ROVs, from their classification and applications to their inherent characteristics and challenges. The obtained knowl-

edge forms a basis for ROV modeling and control design.

According to [1], an ROV's mechanical structure consists of a monitoring camera, a sensor for gathering navigation data, and actuators for directional control. A comparative study [2] found that the physical aspects that affect ROV functions are the accuracy of sensor systems and the thruster designs. The unpredictable nature of underwater currents, drag, and buoyancy dynamics can also have a serious impact on a ROV's performance, complicating model design.

Several studies [3], [4] have identified that ROVs have become crucial for industrial applications, offshore oil and gas exploration, patrolling, and surveillance. Therefore, its control system should focus on position tracking and station keeping in the presence of parameter and environmental uncertainties, addressing the following issues.

The subsequent section explores the mathematical models that serve as the basis for designing such control systems. These models are crucial for comprehending and predicting the behavior of ROVs under varying operating conditions.

II   Mathematical Modelling

Remotely operated vehicles require mathematical models for various purposes, including control system design, simulation, and performance analysis.

Thor I. Fossen [5] provided a complete description of the fundamentals of mathematical modeling for marine vehicles. In his book, ROV was represented as a single rigid body (SRB) by considering it as a solid mass with no internal movement or deformation. The SRB model has drastically simplified the modeling while capturing the essential dynamics of the system.

From a kinematic point of view, ROVs have six degrees of freedom (DoFs).

However, the orientation expressed in the rotation angles could eventually lead to the singularity. To solve this issue, [6] proposed the quaternion representation. The dynamics was derived based on classical physics laws: Newton's Second Law and Euler-Lagrange equation, forming the set of nonlinear equations. The study [7] simplified the equations and represented them in a matrix form.

However, several sources have established that some aspects of the ROV dynamics require empirical estimates due to their complex, nonlinear, and coupled nature [5], [8]. For instance, the inertia of the surrounding fluid cannot be neglected when the vessel moves through a viscous medium. Additionally, water damping is another source of nonlinearity that can be approximated as a function of the velocity. Finally, aside from buoyancy and gravity, it is common practice to cancel all other forces acting on a vehicle, although it can also impact the dynamics [8].

Moreover, thruster modeling must be applied to define the desired thrust of each thruster. A recent study by [8] stated that creating an accurate thruster model can be challenging due to the influence of factors such as motor models, hydrodynamic effects, and propeller mapping.

By making these simplifications, the control system cannot independently provide effective control over such uncertain dynamics. As a result, a robust controller design is necessary for precise ROV position tracking.

III   Control Solutions

Controlling a remotely operated vehicle (ROV) is a complex task that involves several processes to stabilize the vehicle and ensure it follows the operator's instructions. To guarantee the system's robustness, it's essential to establish a

control system capable of managing disturbances caused by changes in parameters and the environment.

According to [4], [9], ROV control faces two main challenges: unmodeled elements like added mass and hydrodynamic coefficients, and highly nonlinear dynamics of the underwater environment causing significant disturbances for the vehicle.

One of the most basic approaches for nonlinear control is the inverse dynamics approach [10]. Despite its simplicity, this approach is limited by its reliance on precise model parameters and its inability to handle significant disturbances effectively.

The research on ROV control showed several schemes that can achieve robust stability under variable disturbances. The classical approach applied is sliding mode control (SMC), which was introduced by Utkin [11]. SMC is an effective way to address the issues mentioned above and is, therefore, a feasible option for controlling underwater vehicles. However, standard SMC introduces high-frequency signals, which can cause actuator switching and consequently decrease its lifetime [12], [13].

Through the application of convex optimization, a balance can be achieved between control performance and actuator longevity, showing promise in enhancing the reliability and efficiency of control systems [14], [15]. This method allows for systematic adjustments of SMC parameters to attain optimal performance, thereby strengthening robustness against disturbances and addressing high-frequency switching issues.

IV   Summary

This literature review comprehensively examined the general characteristics, mathematical modeling, and control solutions for underwater vehicles. The overview identified a gap in the field of robust control for remotely operated vehicles, particularly in dealing with parameter and environmental uncertainties. While the original sliding mode control scheme provided robust stability, it suffered from high-frequency output oscillations. To address this issue, a combination of convex optimization and sliding mode was proposed.

Chapter 3

Mathematical Modelling

Remotely operated vehicles (ROVs) are complex systems that require mathematical models for various purposes, including control system design, simulation, and performance analysis. With accurate mathematical models, ROVs are able to navigate through different underwater terrains and complete control tasks with a good precision. Also, the simulation, based on these models, are suitable to test different work scenarios and detect undesirable ROV's behavior before the physical experiment.

The fundamentals of the modelling for marine vehicles were fully described in Fossen [5]. Using common assumptions, ROV is treated as a single rigid body with six degrees of freedom (DOF). By considering the vehicle as a rigid body, we can simplify the mathematical modeling process while capturing the essential dynamics of the system.

In order to effectively model rigid bodies, it is crucial to consider their kinematic and dynamic properties.

I Notations

Before examining the theory underlying the modeling process, it is crucial to establish clarity on the notations.

In the context of motion with six degrees of freedom (DOF), a set of six independent coordinates is defined within the coordinate frame: three for translational directions (surge, sway, and heave) and three for rotational directions (roll, pitch, and yaw), as shown in Fig. 1.
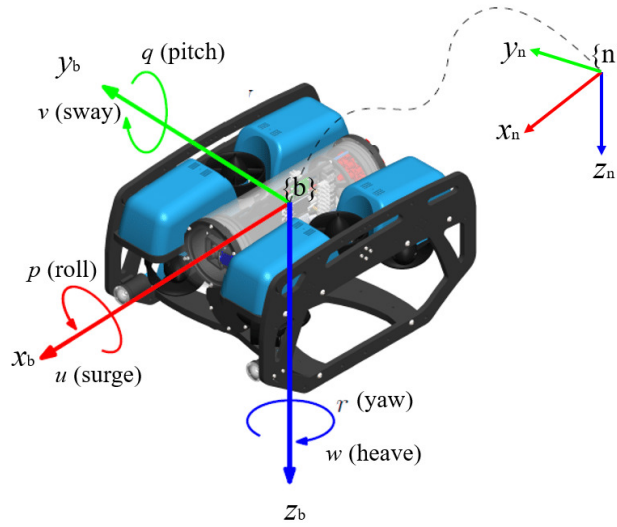
Fig. 1. Illustration of the Six Degrees of Freedom (DOF) for a Marine Vehicle. Adopted from [16]

The linear position of the body in three-dimensional space is defined as $\mathbf{r} = [r_x, r_y, r_z]^\top$, representing translations along the x, y, and z axes, respectively.

While the orientation of the body can be expressed using Euler angles, this approach can lead to singularities when the sway angle approaches $\pm 90°$. To overcome this limitation, quaternions provide a more robust representation by introducing redundancy. A quaternion, represented in scalar-first form, is defined

as

$$\mathbf{q} = q_0 + q_1 i + q_2 j + q_3 k = [q_0, q_1, q_2, q_3]^\top \tag{3.1}$$

This quaternion-based representation avoids the singularities associated with Euler angles and ensures a smooth and continuous description of orientation in three-dimensional space.

The velocity vectors can be defined separately: $\mathbf{v} = [v_x, v_y, v_z]^\top$ for translation along the x, y, and z axes, and $\boldsymbol{\omega} = [\omega_x, \omega_y, \omega_z]^\top$ for rotation around the same axes. Similarly, this applies to linear forces and torques, where $\mathbf{f}$ represents the linear forces and $\boldsymbol{\tau}$ represents the torques acting on the body.

TABLE I
Notations for Motion Parameters in ROV Modeling

Symbol	Description	Dimensionality
r	Linear position vector	$\mathbb{R}^3$
q	Angular position (orientation) vector	$\mathbb{R}^4$
v	Linear velocity vector	$\mathbb{R}^3$
ω	Angular velocity vector	$\mathbb{R}^3$
f	Vector of linear forces	$\mathbb{R}^3$
τ	Vector of torques	$\mathbb{R}^3$

For convenience, it is desirable to define combined vectors for positions, velocities, and forces as follows:

$$\bar{r} = \begin{bmatrix} r \\ q \end{bmatrix}, \quad \bar{v} = \begin{bmatrix} v \\ \omega \end{bmatrix}, \quad \bar{f} = \begin{bmatrix} f \\ \tau \end{bmatrix}$$

To manipulate the obtained vectors, it is necessary to define cross product operators. For vectors in $\mathbb{R}^3$, the cross product is represented by multiplication with a skew-symmetric matrix $S(\lambda)$:

$$S(\lambda) = \begin{bmatrix} 0 & -\lambda_3 & \lambda_2 \\ \lambda_3 & 0 & -\lambda_1 \\ -\lambda_2 & \lambda_1 & 0 \end{bmatrix} \tag{3.2}$$

For vectors in $\mathbb{R}^6$, the cross product operator $\bar{\times}^*$ is defined as:

$$x\bar{\times}^* = \begin{bmatrix} S(x_2) & 0_{3\times 3} \\ S(x_1) & S(x_2) \end{bmatrix} \text{ for } x = \begin{bmatrix} x_1 \\ x_2 \end{bmatrix} \tag{3.3}$$

II   Frames of reference

To accurately determine the movement and forces of the system, it's important to perform calculations within a consistent frame of reference. In the case of an ROV, two coordinate frames are utilized: the earth-fixed frame, which is stationary, and the body-fixed frame, which moves with the vehicle. The body-fixed frame aligns with the vehicle's center of mass and its axes correspond to the vehicle's principal axes of inertia.

The state variables of the rigid body expressed in the body-fixed frame would be denoted by ^{B} and in the earth-fixed frame by ^{N}.

III   Kinematics

Kinematics describes the motion of the marine vehicle without considering the forces acting upon it. In order to describe kinematic motion of the body, it is necessary to find relation between velocities in two coordinate frames. This relation can be represented with linear transformations as:

$$\dot{\bar{r}}^N = J(\bar{r}^N)\bar{v}^B$$

$$\text{where } J(\bar{r}^N) = \begin{bmatrix} R(\bar{r}^N) & 0_{3\times3} \\ 0_{4\times3} & T(\bar{r}^N) \end{bmatrix} \tag{3.4}$$

The rotational matrix R and the transformation matrix T using quaternion representation 3.1 can be expressed as follows:

$$R(q) = \begin{bmatrix} 1 - 2\left(q_2^2 + q_3^2\right) & 2\left(q_1q_2 - q_3q_0\right) & 2\left(q_1q_3 + q_2q_0\right) \\ 2\left(q_1q_2 + q_3q_0\right) & 1 - 2\left(q_1^2 + q_3^2\right) & 2\left(q_2q_3 - q_1q_0\right) \\ 2\left(q_1q_3 - q_2q_0\right) & 2\left(q_2q_3 + q_1q_0\right) & 1 - 2\left(q_1^2 + q_2^2\right) \end{bmatrix} \tag{3.5}$$

$$T(q) = \frac{1}{2} \begin{bmatrix} -q_1 & -q_2 & -q_3 \\ q_0 & -q_3 & q_2 \\ q_3 & q_0 & -q_1 \\ -q_2 & q_1 & q_0 \end{bmatrix} \tag{3.6}$$

IV   Dynamics

The Newton-Euler approach is commonly used to describe the dynamics of marine vehicles. This approach relates the applied forces and moments to the

vehicle's linear and angular accelerations. The general equation of motion using the Newton-Euler approach in the body-fixed frame can be written as:

$$M\dot{\bar{v}}^B + \bar{v}^B \bar{\times}^* M\bar{v}^B = \bar{f}^B \tag{3.7}$$

where M represents the inertia matrix of the rigid body.

The equation above can be further transformed into standard manipulator equation form:

$$M_B\dot{\bar{v}}^B + C_B(\bar{v}^B)\bar{v}^B = \bar{f}^B \tag{3.8}$$

where: M_B the rigid body mass matrix $\in \mathbb{R}^{6x6}$

     C_B the rigid body Coriolis and centripetal forces' matrix $\in \mathbb{R}^{6x6}$

Nevertheless, some additional terms should be included in the equation to determine the specifics of the ROVs model. These terms comprise added mass, which represents the inertia of the surrounding fluid, the shift of the center of buoyancy due to changes in trim and heel angles, and damping effects. By incorporating these terms into the manipulator equation derived from the Newton-Euler approach, the model becomes more accurate and reflects the natural behavior of the ROV.

A.   *Center of Gravity and Center of Buoyancy*

Due to the robust design of the marine vehicles, the center of buoyancy (COB) is usually aligned with the center of mass (COM), but placed higher. This shift between centers causes torque acting against the capsizing (Fig. 2).
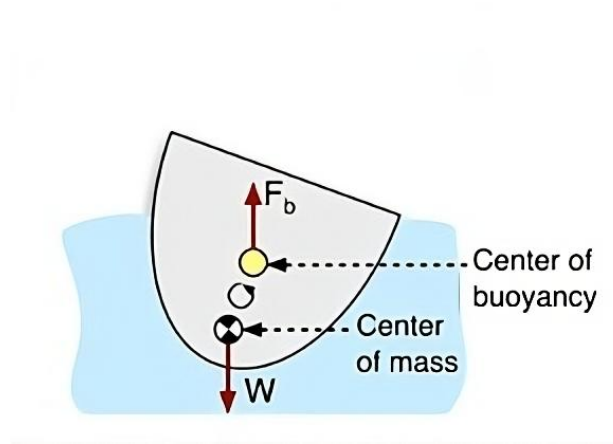
Fig. 2. Schematic representation of the marine vehicle showing the center of buoyancy (COB) and the center of mass (COM). Adopted from [17]

If we place the origin of the body frame at the center of mass, the mass matrix can be expressed as:

$$M_B = \begin{bmatrix} mI_{3\times3} & -mS\left(r_G^B\right) \\ mS\left(r_G^B\right) & I_0 \end{bmatrix} \tag{3.9}$$

where r_G^B is the vector of the gravity center in the body frame, that is eventually a zero vector.

B. Concept of added mass

Since the vehicle moves in a viscous environment, we can not neglect the inertia of the surrounding liquid. To compensate added mass effect, it is necessary to add two components into dynamics equation: the added mass and the Coriolis forces acting on the added mass.

We can define vector of dynamical parameters of our body as:

$$f_{\dot{v}} \triangleq \frac{\partial \bar{f}}{\partial \dot{\bar{v}}} \tag{3.10}$$

Consequently, the added mass matrix M_A and the Coriolis forces matrix for added mass $C_A(\bar{v}^B)$ can be expressed as:

$$M_A = \begin{bmatrix} A_{11} & A_{12} \\ A_{21} & A_{22} \end{bmatrix} = -\operatorname{diag}\{f_{\dot{v}}\}, \text{where } A_{ij} \in \mathbb{R}^{3x3} \qquad (3.11)$$

$$C_A(\bar{v}^B) = \begin{bmatrix} 0_{3\times3} & -S\left(A_{11}v^B + A_{12}\omega^B\right) \\ -S\left(A_{11}v^B + A_{12}\omega^B\right) & -S\left(A_{21}v^B + A_{22}\omega^B\right) \end{bmatrix} \qquad (3.12)$$

The values of dynamical parameters are usually determined empirically. Therefore, the error on M_A and C_A can be quite large, and we will not consider these matrices in our model implementation for the control design.

C. Hydrodynamic Damping

Generally, the dynamics of underwater vehicles can be highly nonlinear and coupled. Nevertheless, during the slow non-coupled motion the damping can be approximated to linear and quadratic damping:

$$D(\bar{v}^B) = -K_0 - K_1|\bar{v}^B| \qquad (3.13)$$

The appropriate values of damping coefficients for vectors K_0 and K_1 can be discovered through several experiments.

D. Restoring forces

The common sense is to neglect all other forces acting on the vehicle except buoyancy and gravity. Although the motion of the current can also affect the dynamics, it is unpredictable and highly nonlinear, which makes it easier to

compensate through control.

The weight of the body is defined as: $\mathbf{W} = \mathbf{mg}$, where m is the vehicle's mass and g is the gravity acceleration. The buoyancy force is defined as: $\mathbf{B} = \rho \mathbf{g} \mathbf{V}$, where ρ is the water density and V the volume of fluid displaced by the vehicle.

By transforming the weight and buoyancy force to the body-fixed frame, we get:

$$f_G\left(\bar{r}^N\right) = R^\top\left(\bar{r}^N\right)[0,0,W]^\top \tag{3.14}$$

$$f_B\left(\bar{r}^N\right) = -R^\top\left(\bar{r}^N\right)[0,0,B]^\top \tag{3.15}$$

Therefore, overall restoring force and moment vector is defined as:

$$g(\bar{r}^N) = -\begin{bmatrix} f_G(\bar{r}^N) + f_B(\bar{r}^N) \\ r_G^B \times f_G(\bar{r}^N) + r_B^B \times f_B(\bar{r}^N) \end{bmatrix} \tag{3.16}$$

where r_B^B is the vector of the buoyancy center in the body frame.

E. Matrix representation

Combining all the equations above, the final representation of the system dynamics is:

$$M\dot{\bar{v}}^B + C(\bar{v}^B)\bar{v}^B + D(\bar{v}^B)\bar{v}^B + g(\bar{r}^N) = \bar{f}^B \tag{3.17}$$

where: $\quad M \quad = M_B + M_A$

$\quad\quad\quad C(\bar{v}^B) \quad = C_B(\bar{v}^B) + C_A(\bar{v}^B)$

V   Thrusters modelling

The force and moment vector produced by the thruster are typically represented by a complex nonlinear function $f(\bar{v}^B, V, u)$, which depends on the vehicle's velocity vector $\bar{v}^B$, the power source voltage V, and the control variable u.

However, expressing such a nonlinear relationship directly can be challenging in practical applications. As a result, some authors propose a simpler approach [18]:

$$\bar{f}^B = T\phi(u) \tag{3.18}$$

where: T the thrust configuration matrix, which maps body torques to truster forces $\in \mathbb{R}^{6xn}$

$\phi(u)$ the DC-gain transfer function, which defines relation between PWM signal and output force $\in \mathbb{R}^{nxn}$

VI   Summary

This chapter provides a comprehensive overview of essential concepts and equations crucial for understanding the kinematics and dynamics of ROVs.

Notation

ROVs have six degrees of freedom (DOF), which include three for translation and three for rotation. The use of quaternions to represent orientation helps to avoid singularity issues.

Frame of reference

There are two coordinate frames: the earth-fixed frame and the body-fixed frame. State variables are denoted by $_B$ in the body-fixed frame and $_N$ in the earth-fixed

one.

Kinematics

The motion of a marine vehicle, without considering external forces, is expressed in terms of velocities for two coordinate frames (3.4):

$$\dot{\bar{\mathbf{r}}}^{\mathbf{N}} = \mathbf{J}(\bar{\mathbf{r}}^{\mathbf{N}})\bar{\mathbf{v}}^{\mathbf{B}}$$

Dynamics

The Newton-Euler approach is used to describe the dynamics of ROV by relating applied forces and moments to linear and angular accelerations (3.17):

$$\mathbf{M}\dot{\bar{\mathbf{v}}}^{\mathbf{B}} + \mathbf{C}(\bar{\mathbf{v}}^{\mathbf{B}})\bar{\mathbf{v}}^{\mathbf{B}} + \mathbf{D}(\bar{\mathbf{v}}^{\mathbf{B}})\bar{\mathbf{v}}^{\mathbf{B}} + \mathbf{g}(\bar{\mathbf{r}}^{\mathbf{N}}) = \bar{\mathbf{f}}^{\mathbf{B}}$$

Additional terms like added mass, center of buoyancy, and damping effects enhance model accuracy.

Thruster modelling

The complex relationship between thruster force and control variables is simplified using a thrust configuration matrix T and a DC-gain transfer function $\phi(u)$ (3.18):

$$\bar{\mathbf{f}}^{\mathbf{B}} = \mathbf{T}\phi(\mathbf{u})$$

The mathematical models developed in this chapter lay the foundation for designing control systems. By accurately capturing the dynamics and kinematics of ROVs, these models enable precise navigation underwater. The next chapter will implement effective control strategies and enhance the performance of ROVs in various scenarios.

Chapter 4

Methodology

The development of a robust control system for underwater robots hinges on a comprehensive understanding of system dynamics and control objectives. This chapter explores control design for underwater robots, focusing on the application of sliding mode control to address challenges in marine environments. By integrating robust control strategies, the aim is to enhance the stability, accuracy, and responsiveness of underwater robotic systems operating in dynamic and unpredictable conditions.

I   Design Considerations

This section provides an introduction to control systems, starting with defining objectives that serve as a foundation for understanding subsequent topics.

A.   Control Objectives

The main idea of the control system design is to choose such control input u which meets the desired performance specifications while ensuring stability.

Underwater robots require precise control systems to navigate and operate effectively in challenging marine environments. These control objectives are crucial for ensuring the robot's stability, accuracy, and responsiveness:

- Position and Orientation Tracking: The robot must accurately follow a desired trajectory, maintaining its position and orientation as intended.

- Disturbance Rejection: The robot should be able to withstand external disturbances, such as ocean currents, waves, and sensor noise, to maintain stable tracking performance.

- Robustness: The control system should be robust to uncertainties in the robot's dynamics and environmental conditions, ensuring reliable operation even in unpredictable situations.

- Real-Time Implementation: The control algorithm should be computationally efficient and able to run in real-time on the robot's embedded system, enabling prompt and effective responses to changing conditions.

Next, let us discuss the challenges posed by uncertainties in control system modeling, which must be understood before diving into advanced control techniques.

B. Model Uncertainties

The estimated model dynamics may not perfectly match the actual system behavior due to imprecise parameter estimates caused by simplified dynamics and external factors. Two primary types of modeling inaccuracies are defined by J. Slotine and W. Li [19]:

1. Structured (or parametric) uncertainties : associated with errors in the terms included in the model

2. Unstructured uncertainties (or unmodeled dynamics) : linked to inaccuracies in the system's order

Recalling dynamics of ROV, following parameters may have some imprecision:

- **Body parameters**. The mass matrix M_B and the matrix of Coriolis forces C_B may unknown due to uncertain values of mass m and inertia matrix I_0.

- Coefficients of **viscous damping** D. The values for linear and quadratic terms are defined empirically.

- **Restoring forces** g. Specifically, water density ρ is environment dependent and whole body volume ∇ is hard to calculate with proper accuracy.

- **Added mass parameters** M_A and C_A. They cannot be calculated directly and will be excluded in future calculations.

Further, the approximated value of the parameter x is represented as $\hat{x}$, while the difference between this approximation and the actual value is defined as $\tilde{x} = \hat{x} - x$. Instead of the omitted terms, we will incorporate a common disturbance term δ.

In this way, the dynamics in equation 3.17 takes the following form:

$$M_B \dot{\bar{v}}^B + C_B(\bar{v}^B)\bar{v}^B + D(\bar{v}^B)\bar{v}^B + g(\bar{r}^N) + \delta = T\phi(u) \qquad (4.1)$$

C.   Thruster Mapping Approximation

As stated before, thruster mapping is defined through the configuration matrix T and the DC-gain transfer function $\phi(u)$. However, $\phi(u)$ can be highly nonlinear and voltage dependent. Let us examine the general function $\phi(u)$ shown in Fig. 3.
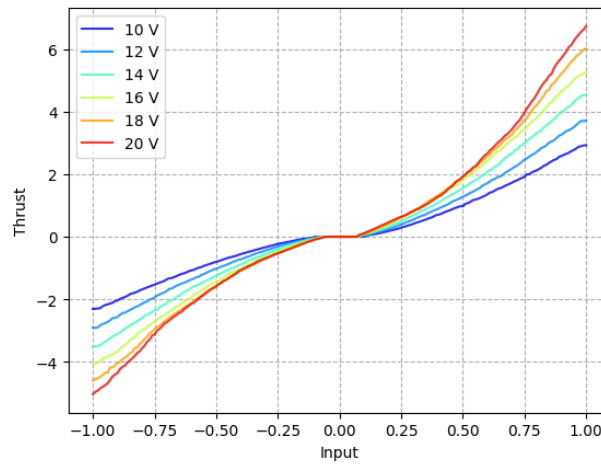
Fig. 3. Relationship Between Thrust Output and Pulse Width Modulation (PWM) Signal for ROV Thrusters

It is suggested to use a third-order polynomial to model the transfer function above. This approach is deemed suitable due to the general shape of the PWM to thrust relation.

The approximated function is expressed as

$$\hat{\phi}(u) = k\phi_0(u) \tag{4.2}$$

where: k the scaling coefficient

$\phi_0(u)$ the nominal third-order polynomial

The value of k must be between $k_{min} = 0.4$ and $k_{max} = 1$ to cover the entire range. (Fig. 4).
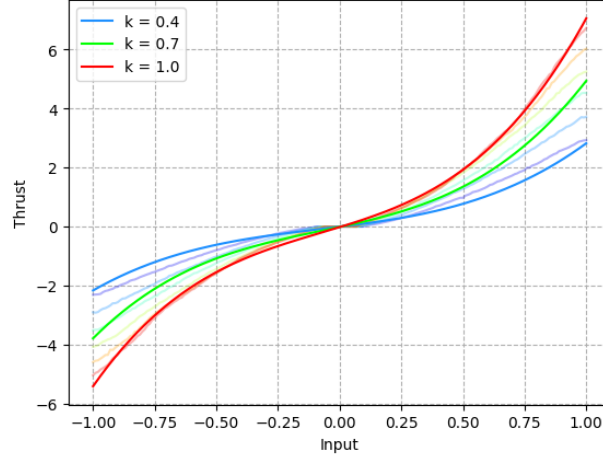
Fig. 4. Approximation Model for Thruster Mapping in ROV Control Systems

Thus, the thruster mapping takes the form:

$$\hat{\bar{f}}^B = T\hat{\phi}(u) = kT\phi_0(u) = B\phi_0(u) \tag{4.3}$$

D. *Approximated System Dynamics*

By taking into account the impact of both dynamic approximations and disturbances, we can obtain the following dynamics of the system:

$$M_B\dot{\bar{v}}^B + C_B(\bar{v}^B)\bar{v}^B + D(\bar{v}^B)\bar{v}^B + g(\bar{r}^N) + \delta = B\phi_0(u) \tag{4.4}$$

For the sake of simplicity, we omit some redundant notations: $*_B$, $\bar{*}$, $*^B$ and $*^N$. However, the meaning behind these notations remains valid, whereas the formulas become more comprehensible.

Additionally, let us describe the internal and external forces acting on the body using the single nonlinear term $h(r, v)$:

$$h(r, v) = C(v)v + D(v)v + g(r) \tag{4.5}$$

Finally, the approximated system dynamics equation is defined as:

$$M\dot{v} + h(r, v) + \delta = B\phi_0(u) \tag{4.6}$$

E. Summary

To summarize, the main objective of the underwater control system is to accurately follow the desired trajectory, even in the presence of external disturbances and uncertainties. The ultimate goal is to make sure that the tracking error approaches zero as time progresses towards infinity.

As was previously mentioned, control systems can be negatively impacted by modeling nonlinear dynamics. Therefore, any practical design must handle them explicitly. Inverse dynamics control can be a good starting point for deriving complex nonlinear control approaches, as it addresses the nonlinearities present in the system.

II   Inverse dynamics

The nonlinear control method, known as inverse dynamics, tracks a trajectory by calculating the joint actuator torques required to achieve a specific trajectory. This approach relies on exact cancellation of nonlinearities in the robot equation of motion.

The concept of inverse dynamics control is closely linked to solving the inverse dynamics problem. By appropriately inverting the dynamic model, a control law can effectively cancel out the nonlinear dynamics, isolate the interactions between the controlled variables, and specify the time characteristics of the decay of task errors

A.   Virtual Control

To simplify the control process, we can define a virtual control input ν, which is related to the actual control input $\mathbf{u}$ as:

$$\nu = \phi_0(u) \tag{4.7}$$

It is important to note that there exists an inverse relation between the actual control input and the virtual control input, namely $u = \phi_0^{-1}(\nu)$. This inverse relation will allow us to easily switch back and forth between the actual and virtual control inputs as needed.

B.   Control Law Design

Recalling the approximated dynamics equation 4.6, we can design the following virtual control law to linearize the system:

$$\nu = B^+(Ma + h(r,v)) \tag{4.8}$$

while the outer-loop control a is designed as a proportional-derivative (PD) controller:

$$a = \dot{v}_{des} - K_p\tilde{r} - K_d\tilde{v} \tag{4.9}$$

The equation 4.8 becomes more complex when system parameters and disturbances are unknown:

$$\nu = \hat{B}^+(\hat{M}a + \hat{h}(r,v)) \tag{4.10}$$

Substitution to the dynamics yields:

$$\dot{v} = M^{-1}(B\hat{B}^+ h(r,v) - \hat{h}(r,v) - \delta) + M^{-1}B\hat{B}^+\hat{M}a \tag{4.11}$$

C. Error Analysis

In terms of tracking error $e = \tilde{r}$, we can design the following system:

$$e = \tilde{r}$$
$$\dot{e} = \tilde{v}$$
$$\ddot{e} = \dot{\tilde{v}} = \tag{4.12}$$
$$= \dot{v}_{des} - \dot{v} =$$
$$= \dot{v}_{des} - M^{-1}(B\hat{B}^+ h - \hat{h} - \delta) + M^{-1}B\hat{B}^+\hat{M}(\dot{v}_{des} - K_p e - K_d \dot{e})$$

Hence, the error dynamics can be represented in the form of a second-order differential equation as:

$$\ddot{e} + A_1\dot{e} + A_0 e = (W - I)\dot{v}_{des} - M^{-1}(B\hat{B}^+ h - \hat{h} - \delta) =$$
$$= d(e, \dot{e}, \dot{v}_{des}) \tag{4.13}$$

with $W = M^{-1}B\hat{B}^+\hat{M}$, $A_0 = WK_p$ and $A_1 = WK_d$.

In state-space form, we can express the error dynamics as:

$$\dot{x} = Ax + Bd \tag{4.14}$$

where

$$x = \begin{bmatrix} e \\ \dot{e} \end{bmatrix}, \quad A = \begin{bmatrix} 0_{6\times6} & I_{6\times6} \\ -A_0 & -A_1 \end{bmatrix}, \quad B = \begin{bmatrix} 0_{6\times6} \\ I_{6\times6} \end{bmatrix}$$

The analytical solution of the state-space equation is given by:

$$x(t) = e^{At}x(0) + \int_0^t e^{A(t-\tau)}Bd(\tau)\,d\tau \tag{4.15}$$

To find the bounds on the error, we assume that $(e, \dot{e}, \dot{v}_{des})$ is bounded, i.e., $\|d\| \leq D$, and derive:

$$\|x(t)\| \leq Ce^{-\alpha t}\|x(0)\| + \int_0^t Ce^{-\alpha(t-\tau)}\|B\|D\,d\tau \tag{4.16}$$

Evaluating the integral, we get:

$$\|x(t)\| \leq Ce^{-\alpha t}\|x(0)\| + \|B\|DC\left[\frac{1 - e^{-\alpha t}}{\alpha}\right] \tag{4.17}$$

As $t \to \infty$, the exponential terms decay to zero, and we get:

$$\|x(t)\| \leq \frac{C\|B\|D}{\alpha} \tag{4.18}$$

Since $x = \begin{bmatrix} e \\ \dot{e} \end{bmatrix}$, the error e is bounded by:

$$\|e\| \leq \frac{\|d\|}{\lambda_{min}(A_0)} \tag{4.19}$$

where $\lambda_{min}(A_0)$ is the minimum eigenvalue of A_0.

D.   Summary

The inverse dynamics technique, while effective in theory, presents several challenges in practical applications:

- **Undefined or Large Error Bounds**: The error bounds can be large or undefined if $\dot{v}_{des}$ is not properly bounded.

- **Difficulty in Tuning**: The parameters K_p and K_d require careful tuning to achieve desired performance.

- **Lack of Robustness**: The method is not robust to parameter uncertainties and external disturbances.

As a result, the inverse dynamics technique may not be the best option for effectively controlling underwater systems. Further we introduce sliding mode control, which is a robust control technique that can achieve desired control objectives in the presence of uncertainties.

III   Sliding Mode

As discussed before, there are several robust controller designs available. However, the sliding mode approach, suggested by Vadim Utkin in the late 1970s, is highly regarded as the most sophisticated and frequently implemented one [11].

Sliding mode control (SMC) is a nonlinear control method that guarantees robust control of systems with uncertainties and disturbances. This technique involves developing a sliding surface within the state space and directing the system's trajectory to slide along this surface (Fig. 5).

Compared to other nonlinear control methods, SMC is a relatively straight-forward solution to implement with a basic understanding of system dynamics and sliding surface design. SMC provides a fast transient response due to the sliding dynamics, which makes it possible to track desired references or trajectories quickly.
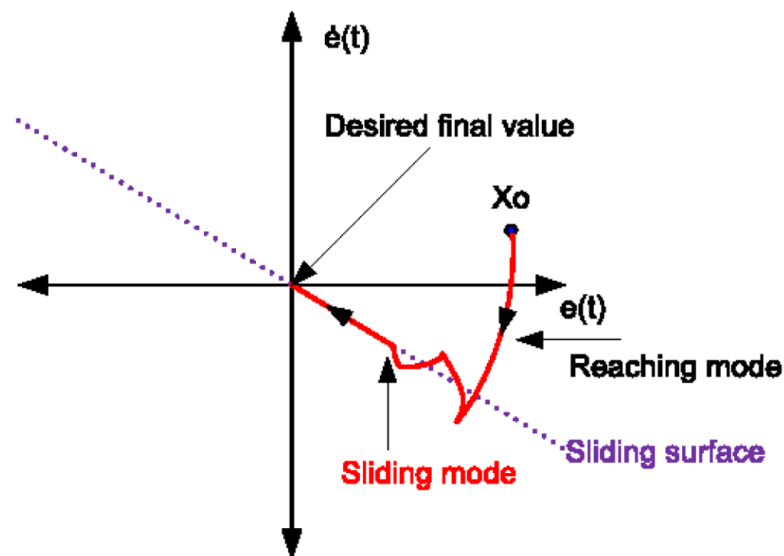
Fig. 5. General Schematic of Sliding Mode Control (SMC). Adopted from [20]

A.   Sliding Surface Design

In sliding mode control, a sliding surface is a hyperplane in the state space that defines the desired system behavior. The aim of the control is to force the system's trajectory to slide along this surface. As long as the control law is in effect, the system's trajectory will stay on the sliding surface once it reaches it (Fig. 6).
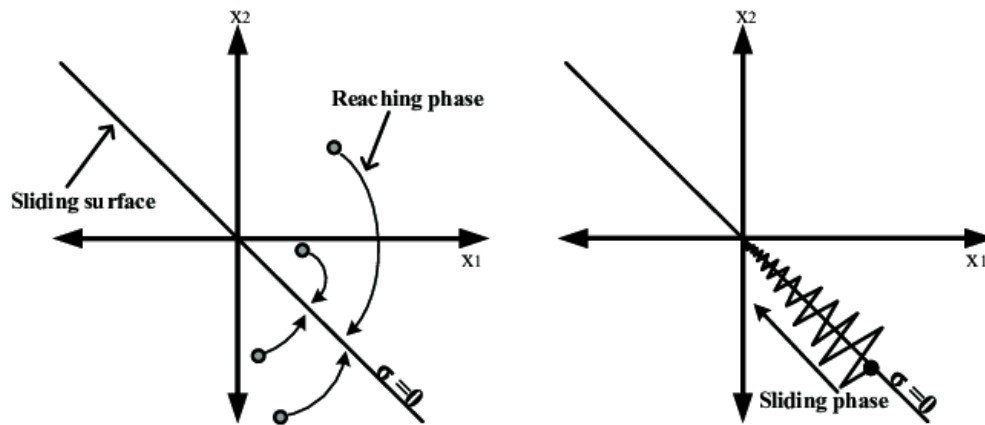
Fig. 6. Phases of Sliding Mode Control: Reaching Phase and Sliding Phase. Adopted from [21]

The design of the sliding surface is critical for the performance of the SMC system. The sliding surface should be:

- Reachable: The system's trajectory should be able to reach the sliding surface in a finite amount of time.

- Invariant: The system will stay on the sliding surface as long as the control law is in effect once its trajectory reaches it.

- Attractive: The control law should attract the system's trajectory to the sliding surface and keep it there.

In order to satisfy the conditions above, the sliding surface is designed to be an invariant set. Invariant sets are sets of states in the state space that, once entered, cannot be exited under the action of the control law.

B.   *Sliding Condition*

In the state space $\mathbb{R}^n$, let us define the time-varying surface given by scalar equation $\mathbf{s}(\mathbf{r}, \mathbf{t})$:

$$\mathbf{s}(\mathbf{r}, \mathbf{t}) = (\frac{d}{dt} + \lambda)^{n-1} \tilde{r} \tag{4.20}$$

where n denotes the system's order and λ is a positive scalar.

In order to ensure convergence of $\mathbf{s}(\mathbf{r}, \mathbf{t})$ along all system trajectories in finite time, let us define Lyapunov candidate $\mathbf{V} = \mathbf{s^2}$ as the squared distance to the surface.

The sliding condition can then be formulated accordingly:

$$\frac{dV}{dt} < -\eta \sqrt{V} \quad \text{or} \quad \frac{1}{2}\frac{d}{dt}\|s\|^2 = s^T \dot{s} < -\eta\|s\| \tag{4.21}$$

where $\eta > 0$ defines the rate of convergence to the sliding surface.

When the sliding condition is satisfied, the surface becomes an invariant set and implies convergence to $\tilde{\mathbf{r}}$, since the system described by the differential equation:

$$s = (\frac{d}{dt} + \lambda)^{n-1} \tilde{r} = 0 \tag{4.22}$$

is inherently stable and remains at the equilibrium point $\tilde{\mathbf{r}} = \mathbf{0}$.

Applying such transformation yields a new representation of the tracking performance:

$$s \to 0 \Rightarrow \tilde{r} \to 0 \tag{4.23}$$

In other words, tracking $\mathbf{r}$ is the same as staying on the sliding surface. It is thus possible to replace the tracking problem of the n-dimensional vector $\mathbf{r}$ with a first order stabilization problem in $\mathbf{s}$.

C. Control Law Design

The control input $\mathbf{a}$ comprises two distinct components: nominal control $\mathbf{a_n}$, and an additional robust part $\mathbf{a_s}$:

$$a = a_n + a_s \tag{4.24}$$
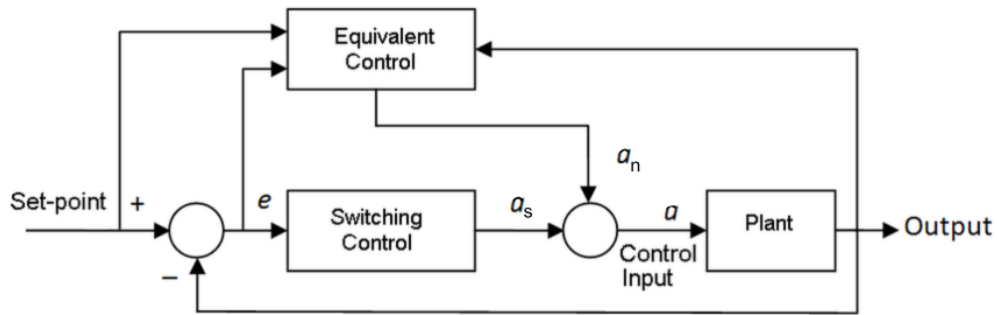
Fig. 7. Control Scheme for Sliding Mode Control (SMC) in ROVs

The nominal control $\mathbf{a_n}$ aims to compensate for the system's dynamics, while the robustifying component $\mathbf{a_s}$ is designed to enhance the controller's stability and performance by providing additional corrective action to counteract uncertainties and disturbances.

To simplify computations, we can use a virtual force f_v:

$$f_v = T\nu \tag{4.25}$$

which can represent the desired behavior of the system without introducing input uncertainty.

Using the inverse dynamics approach 4.8, we can apply the outer loop con-

troller to partially linearize the system with model estimates:

$$\hat{f} = \hat{k} f_v = \hat{M} a + \hat{h}(r, v) \tag{4.26}$$

Expressing virtual control input, we obtain:

$$f_v = \frac{\hat{M} a + \hat{h}(r, v)}{\hat{k}} \tag{4.27}$$

Substitution to the dynamics 4.6 yields the equation:

$$\dot{v} = \underbrace{M^{-1}(\frac{k}{\hat{k}}\hat{h}(r, v) - h(r, v) - \delta)}_{F(r,v)} + \underbrace{\frac{k}{\hat{k}}M^{-1}\hat{M}}_{K} a = \tag{4.28}$$
$$= F(r, v) + Ka$$

where the terms $F(r, v)$ and K represent dynamical and inertial uncertainties.

The time derivative of **s** is connected to dynamics as follows:

$$\dot{s} = \dot{\tilde{v}} + \lambda \tilde{v} = a_n - \dot{v} = a_n - F - K(a_n + a_s) = w - Ka_s \tag{4.29}$$

with error function $w(r, v) = (I - K)a_n - F(r, v)$

Substitution to sliding condition 4.21 yields:

$$s^T w - s^T Ka_s \le \|s\| \|w\| - s^T Ka_s \le -\eta \|s\| \tag{4.30}$$

Let us recall that for any symmetric matrix **P**:

$$\sigma_{min}^2 \|x\|^2 \le \|x^T Px\| \le \sigma_{max}^2 \|x\|^2 \tag{4.31}$$

with σ_{min} and σ_{max} being the largest and smallest eigenvalues of matrix P.

Thus, we can use property 4.31 to choose the stabilizing control $\mathbf{a_s}$ as:

$$a_s = \frac{\alpha \hat{k}}{\sigma_{min}^2} \hat{M}^{-1} \frac{s}{\|s\|} = \rho \frac{s}{\|s\|} \quad (4.32)$$

where σ_{min} is minimal singular value of M^{-1} which provide:

$$\|s\|\|w\| - s^T K a_s \leq \|s\|\|w\| - k \frac{\alpha}{\sigma_{min}^2 \|s\|} s^T M^{-1} s \leq \|s\|\|w\| - \alpha k \|s\| \quad (4.33)$$

but by definition $k_{min} < k < k_{max}$, therefore

$$\|s\|\|w\| - \alpha k \|s\| \leq \|s\|\|w\| - \alpha k_{min} \|s\| < -\eta \|s\| \quad (4.34)$$

Setting gain α accordingly to:

$$\alpha > \frac{\|w\| + \eta}{k_{min}} \quad (4.35)$$

will satisfy sliding conditions.

The final expression for sliding control:

$$a_s = \begin{cases} \rho \frac{s}{\|s\|}, & \|s\| > 0 \\ 0, & \|s\| = 0 \end{cases} \quad (4.36)$$

In order to reduce chattering, the controller above is effectively smoothed

using the boundary layer:

$$a_s = \begin{cases} \rho \frac{s}{\|s\|}, & \|s\| > \epsilon \\ \rho \frac{s}{\epsilon}, & \|s\| \leq \epsilon \end{cases} \tag{4.37}$$

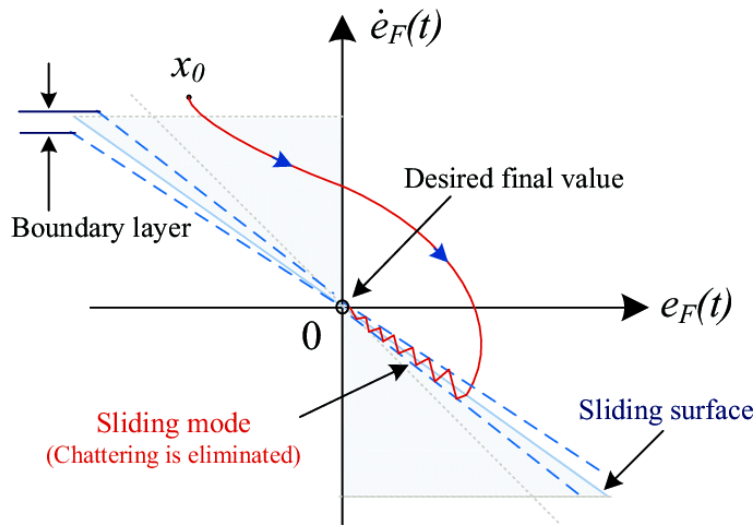where ϵ is the boundary layer thickness.

Fig. 8. Sliding Mode Control Scheme with the Addition of a Boundary Layer to Reduce Chattering. Adopted from [22]

The nominal control a_n can be designed in a form of PD controller:

$$a_n = -K_p \tilde{r}^B - K_d \tilde{v}^B \tag{4.38}$$

The resulting controller is then given as follows:

$$\nu = \hat{B}^+(\hat{M}(a_n + a_s) + \hat{h}(r, v)) \tag{4.39}$$

$$a_n = -K_p \tilde{r} - K_d \tilde{v} \tag{4.40}$$

$$s = \tilde{v} + \lambda \tilde{r} \tag{4.41}$$

$$a_s = \begin{cases} \rho \frac{s}{\|s\|}, & \|s\| > \epsilon \\ \rho \frac{s}{\epsilon}, & \|s\| \leq \epsilon \end{cases} \tag{4.42}$$

D.   Summary

Although sliding mode control has proven to be an effective approach, there are certain drawbacks associated with its use:

- **Chattering**: The control signal can exhibit high-frequency oscillations, potentially causing wear and noise in mechanical systems.

- **Discontinuous Control**: The abrupt switching in the control action can be challenging to implement and may affect actuator performance.

- **Complex Fine-Tuning**: Designing and adjusting the control parameters can be complex and requires expertise.

- **Unlimited Control Input**: The method does not inherently limit the control input, which can result in excessively high control efforts.

Nevertheless, ongoing advancements in control theory and implementation techniques are serving to enhance the value of this method for a range of engineering applications.

While sliding mode control offers robustness in many scenarios, optimization-based control approaches provide an alternative avenue for addressing some of its limitations.

IV   Optimization-based control

Optimization-based control is a highly promising solution for complex control problems, as it endeavors to discover optimal control inputs that fulfill desired performance criteria while also taking system constraints into account.

In modern engineering applications, the pursuit of flexible and versatile control solutions necessitates the use of optimization techniques. These techniques serve to optimize system performance, incorporate constraints and objectives, and facilitate precise tuning and adaptation within complex systems.

A.   *Optimization problem*

Convex optimization involves minimizing a convex objective function over a convex set. Quadratic Programming (QP) is a special type of convex optimization where the objective function is quadratic, and the constraints are linear.

The standard form of a Quadratic Programming problem is given by:

$$\begin{aligned} \underset{x \in R^n}{\text{minimize}} \quad & \frac{1}{2}x^T Q x + c^T x \\ \text{subject to} \quad & Ax \le b, \\ & Ex = d, \end{aligned} \tag{4.43}$$

where: x is the vector of variables to be optimized;

Q is a symmetric positive semidefinite matrix;

c is a vector of linear coefficients;

A, b coefficients and bounds of the inequality constraints;

E, d coefficients and right-hand side of the equality constraints.

The above formulation sets the stage for applying optimization-based control techniques to practical problems.

B.   *Control Law Design*

The core of optimization-based control lies in formulating and solving optimization problems for to the specific dynamics and constraints of the system. Recalling a sliding mode controller 4.39:

$$\hat{M}(a_n + a_s) + \hat{h}(r, v) = \hat{B}\nu$$

This equation represents the controller dynamics, where $\hat{M}$, $\hat{h}$, and $\hat{B}$ are approximated system matrices, a_n represents nominal control inputs, a_s denotes the sliding mode control inputs, and ν represents the virtual control input.

In sliding mode control, a key condition, known as the sliding condition, ensures the system trajectories converge to a specified surface. Mathematically, this condition can be represented as 4.30:

$$s^T K a_s \geq \eta \|s\| + \|s\| \|w\|$$

Here, s represents the sliding surface, K is a gain matrix, η is a positive constant, and w represents disturbance.

General control optimization can be framed as a Quadratic Programming (QP) problem, aiming to minimize a cost function subject to system dynamics and constraints. The basic form of the optimization problem is as follows:

$$
\begin{aligned}
\min_{a_s,\nu} \quad & a_s^T R_a a_s \\
\text{s.t.} \quad & s^T K a_s \geq \eta \|s\| + \|s\| \|w\| \\
& \hat{M} a_s - \hat{B}\nu = -(\hat{M} a_n + h(r,v))
\end{aligned}
\tag{4.44}
$$

However, this basic formulation lacks control bounds. To address this, additional constraints are introduced, ensuring that the control inputs remain within feasible bounds:

$$
\phi_0(u_{min}) \leq \nu \leq \phi_0(u_{max})
\tag{4.45}
$$

Moreover, to alleviate chattering, an uncertainty term d is introduced to the sliding condition. The resulting relaxed sliding condition yields the following optimization problem:

$$
\begin{aligned}
\min_{a_s,\nu,d} \quad & a_s^T R_a a_s + \nu^T R_\nu \nu + \gamma^2 d \\
\text{s.t.} \quad & s^T K a_s \geq \eta \|s\| + \|s\| \|w\| + d \\
& \hat{M} a_s - \hat{B}\nu = -(\hat{M} a_n + h(r,v)) \\
& \phi_0(u_{min}) \leq \nu \leq \phi_0(u_{max})
\end{aligned}
\tag{4.46}
$$

Finally, to smooth the control input and reduce abrupt changes, a penalty term is introduced to penalize large deviations between consecutive control inputs:

$$
\begin{aligned}
\min_{a_s,\nu,d} \quad & a_s^T R_a a_s + \nu^T R_\nu \nu + \gamma_0^2 d + \gamma_1 \|a_s - a_{s(prev)}\| \\
\text{s.t.} \quad & s^T K a_s \geq \eta\|s\| + \|s\|\|w\| + d \\
& \hat{M} a_s - \hat{B}\nu = -(\hat{M} a_n + h(r,v)) \\
& \phi_0(u_{min}) \leq \nu \leq \phi_0(u_{max})
\end{aligned}
\tag{4.47}
$$

C. Summary

Optimization-based control offers a robust framework for addressing complex control problems by leveraging optimization techniques to derive control laws. By formulating control tasks as optimization problems, we can incorporate system dynamics, constraints, and objectives, achieving optimal performance while ensuring robustness and adaptability.

Chapter 5

Implementation

I   System Description

In this chapter, we detail the implementation of the proposed control scheme for the Remotely Operated Vehicle (ROV) using BlueROV Heavy as the testbed.

A.   *BlueROV Heavy*

The BlueROV Heavy is a versatile and robust underwater vehicle equipped with multiple thrusters, sensors, and control units. It is designed for tasks such as underwater exploration, inspection, and research. The primary components of the BlueROV Heavy include:

- **Thrusters**: Eight thrusters provide six degrees of freedom (DOF) for precise maneuvering.

- **Sensors**: Equipped with a variety of sensors, including an IMU (Inertial Measurement Unit), depth sensor, and cameras for navigation and data collection.

- **Control Unit**: An onboard computer system that processes sensor data and executes control algorithms.

The physical layout and the thruster configuration of the BlueROV Heavy, that allows for complex underwater maneuvers, are shown in Figure 9.
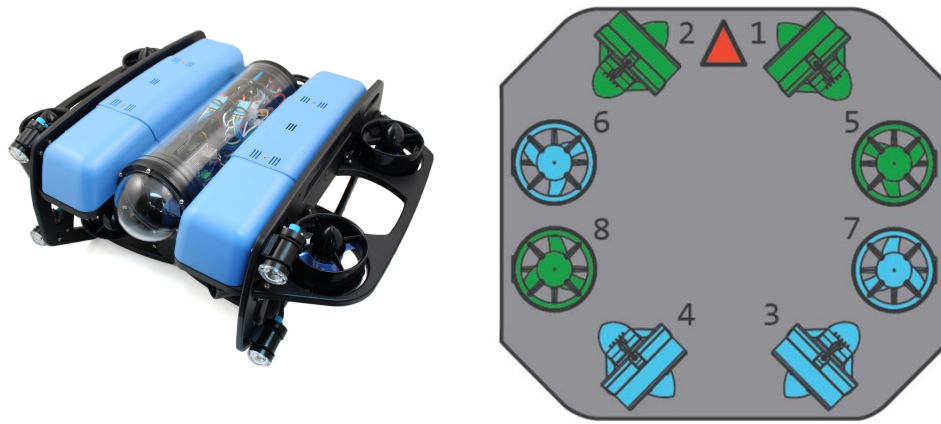

Fig. 9. The BlueROV Heavy and its thruster configuration. The left image shows the basic layout, while the right image highlights the heavy configuration with additional thrusters for enhanced maneuverability. Adopted from [23]

The system parameters required to define the dynamics model (3.17) were obtained from the STL model. These parameters are presented in Tab. II and include values for the mass, weight, buoyancy, center of buoyancy, and moments of inertia.

The viscous damping parameters, which are essential for modeling the resistance forces acting on the ROV, were estimated and are shown in Tab. III.

TABLE II
Initial parameter values for rigid body dynamics and restoring forces

Parameter	Value
Mass	12.5 kg
Weight	125 N
Buoyancy	130 N
Center of Buoyancy	0.1 m
Moment of Inertia (Roll)	0.1 kg m^2
Moment of Inertia (Pitch)	0.1 kg m^2
Moment of Inertia (Yaw)	0.2 kg m^2

TABLE III
Estimated viscous damping parameters

Type	Value
Linear	$[10, 10, 10, 0, 0, 0]^\top$
Quadratic	$[0.1, 0.1, 0.1, 0, 0, 0]^\top$

B. Input Mapping

Input mapping for the BlueROV Heavy utilizes a thrust configuration matrix T and DC-gain transfer function $\phi(u)$ to determine the forces and moments applied by the thrusters.

$$
T = \begin{bmatrix}
-0.7 & -0.7 & 0.7 & 0.7 & 0 & 0 & 0 & 0 \\
0.7 & -0.7 & 0.7 & -0.7 & 0 & 0 & 0 & 0 \\
0 & 0 & 0 & 0 & -1 & 1 & -1 & 1 \\
0 & 0 & 0 & 0 & 0.218 & 0.218 & 0.218 & 0.218 \\
0 & 0 & 0 & 0 & 0.12 & -0.12 & -0.12 & 0.12 \\
0.004 & -0.004 & -0.004 & 0.004 & 0 & 0 & 0 & 0
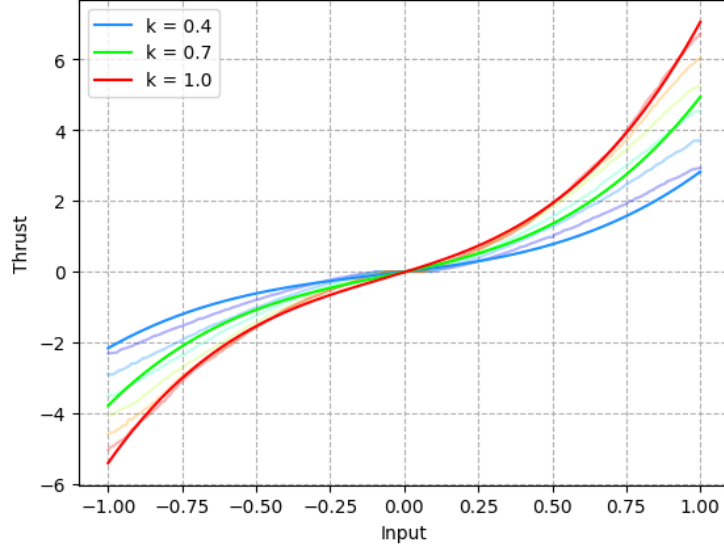\end{bmatrix}
$$

Fig. 10. Thrust characteristics showing the relationship between control input and generated thrust.

The nominal function $\phi_0(u)$ and its inverse $\phi_0^{-1}(\mu)$ are derived based on thruster characteristics, as illustrated in Fig. 10:

$$\phi_0(u_i) = 3.681u_i^3 + 0.839u_i^2 + 2.548u_i - 0.019$$

$$\phi_0^{-1}(\mu_i) = 1.431 \times 10^{-4}\,\mu_i^5 - 9.938 \times 10^{-5}\,\mu_i^4 - 9.064 \times 10^{-3}\,\mu_i^3 -$$
$$- 1.525 \times 10^{-4}\,\mu_i^2 + 0.314\,\mu_i - 0.02$$

II   Code Development

A.   Simulator

The simulation environment for the BlueROV Heavy is built on the open-source MuJoCo physics engine by DeepMind. This provides a reliable platform for testing and validating control strategies under various conditions without the need for real-world testing.

The engine also includes features to simulate environmental factors such as water currents, waves, and obstacles.

B. Codebase

The control system is primarily developed in Python, utilizing a variety of libraries such as NumPy, cvxpy, SciPy, and Matplotlib. These libraries facilitate numerical computations, convex optimization, scientific computing, and data visualization, respectively.

To ensure efficient communication between different components, multi-threading is employed within the codebase. The modular design of the codebase allows for seamless updates and maintenance.
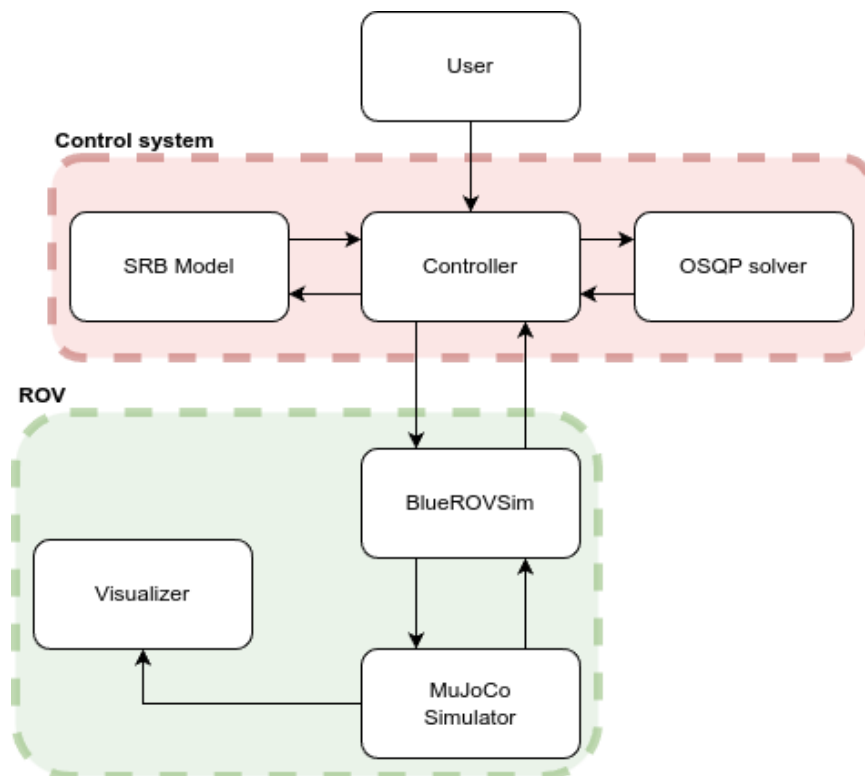

Fig. 11. A schematic overview of the control system architecture, showing the interaction between various components.

The system comprises two main parts (Fig. 11):

- **The Control System**: This involves an SRB modeling module for calculating inverse dynamics, a controller, and an OSQP solver for solving optimization problems.

- **The ROV section**: This includes BlueROVSim, a wrapper over a physics engine for accurate underwater environment simulation, and the MuJoCo Simulator, providing a visual representation of the output.

This setup allows for comprehensive simulation and control of the BlueROV Heavy.

The implementation of the control algorithms was carried out in a structured and modular manner to ensure flexibility and ease of testing.

III   Control System

A.   *Inverse Dynamics*

The inverse dynamics control algorithm calculates the necessary control inputs to achieve desired trajectories by determining forces and moments, and then mapping these to thruster commands.

The control law can be represented by the equation:

$$\nu = B^+(M(\dot{v}_{des} - K_p\tilde{r} - K_d\tilde{v}) + h(r, v))$$

The key components of the inverse dynamics control law include the proportional-derivative (PD) coefficients, which were adjusted to minimize tracking errors, as detailed in Tab. IV.

TABLE IV
PD Coefficients for Inverse Dynamics Control

Parameter	Value
K_p	$[4.0, 4.0, 4.0, 4.0, 4.0, 4.0]^\top$
K_d	$[0.5, 0.5, 3.5, 1.5, 1.5, 1.0]^\top$

B. Sliding Mode Control

Sliding Mode Control (SMC) was implemented to enhance robustness against disturbances and model uncertainties. SMC defines a sliding surface based on desired state variables.

The control force a_s drives the system state towards this surface, maintaining robust performance despite external disturbances:

$$a_s = \begin{cases} \frac{\alpha \hat{k}}{\sigma_{min}^2} \hat{M}^{-1} \frac{s}{\|s\|}, & \|s\| > \epsilon \\ \frac{\alpha \hat{k}}{\sigma_{min}^2} \hat{M}^{-1} \frac{s}{\epsilon}, & \|s\| \leq \epsilon \end{cases}$$

The transition from conventional inverse dynamics to sliding mode control involves the tuning of several key parameters, as detailed in Tab. V.

TABLE V
Fine-tuned parameters for Sliding Mode Control

Parameter	σ_{min}	ϵ	α
Value	1.5	0.5	93.0

C.   *Optimization-based Control*

The optimization-based control scheme dynamically adjusts control parameters using convex optimization techniques. A key aspect of this method is the definition of an objective function and constraints, which are optimized using a convex optimization solver.

The optimization problem is defined as:

$$\min_{a_s,\nu,d} \quad a_s^T R_a a_s + \nu^T R_\nu \nu + \gamma_0^2 d + \gamma_1 \|a_s - a_{s(prev)}\|$$

$$\text{s.t.} \quad s^T K a_s \geq \eta\|s\| + \|s\|\|w\| + d$$

$$\hat{M}a_s - \hat{B}\nu = -(\hat{M}a_n + h(r,v))$$

$$\phi_0(u_{min}) \leq \nu \leq \phi_0(u_{max})$$

Tab. VI lists the parameters used in the optimization process.

TABLE VI
Parameters for Optimization-based Control

Parameter	Value
R_a	$I_{6\times6}$
R_u	$0.01 \cdot I_{8\times8}$
γ_0	0.3
γ_1	0.2
u_{min}	-1.0
u_{max}	1.0
$\|w\|_{max}$	37.0
K_{max}	$15.0 \cdot I_{6\times6}$

Chapter 6

Evaluation and Discussion

In this chapter, the performance assessment of the proposed control strategies for the BlueROV Heavy is presented. This includes the examination of position tracking, the impact of disturbances, and the comparison of different control methods in terms of accuracy and energy consumption.

In order to evaluate the control strategy discussed in Chapter 4, a point-to-point control routine was applied to the controller under small disturbances and uncertainties related to the system parameters. Experiments were conducted to test the control method, and the following are the results of these experiments.

I   Position Tracking

Position tracking is a critical metric for evaluating the effectiveness of control systems. The ability to follow a predefined trajectory with minimal deviation ensures that the ROV can perform precise maneuvers necessary for underwater tasks such as inspection and data collection.

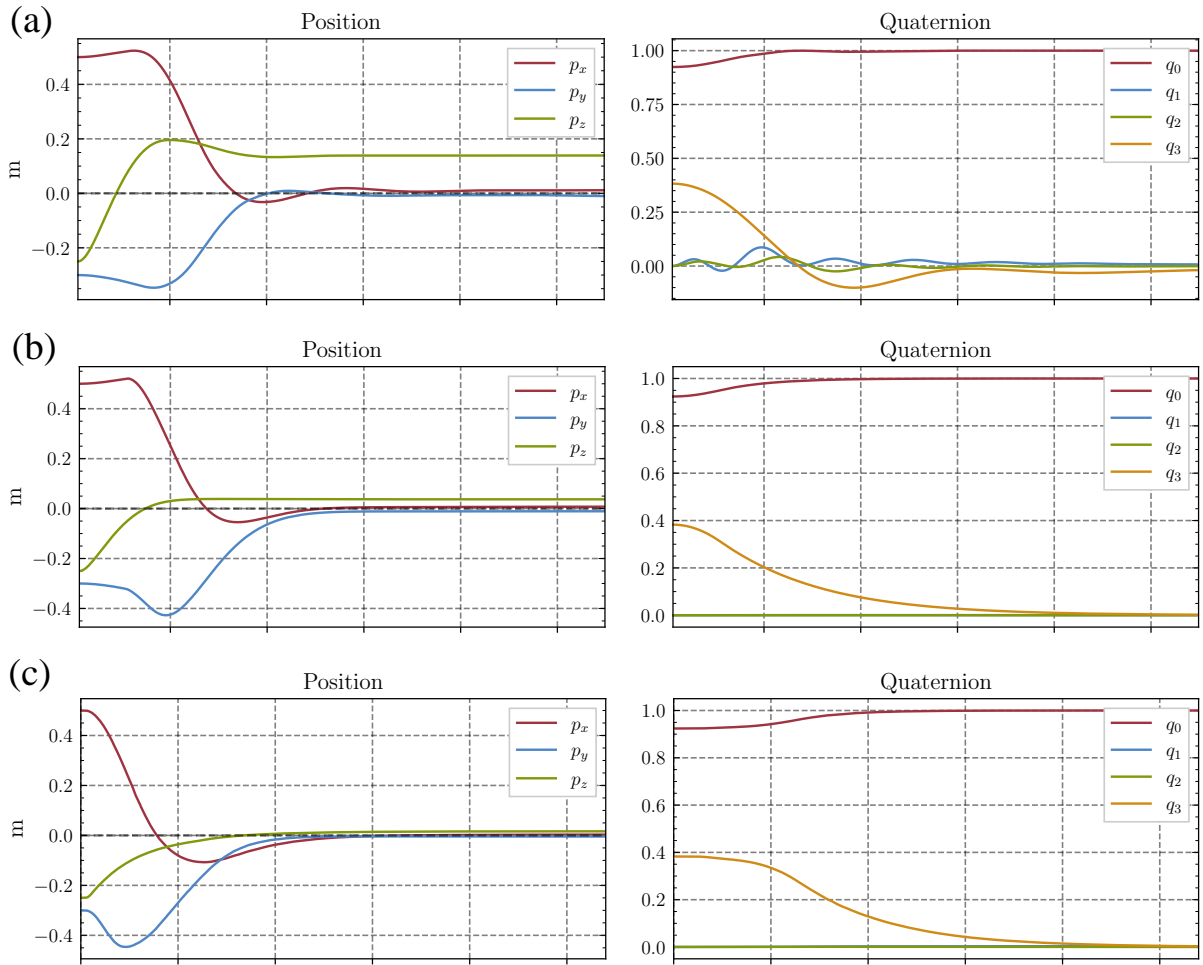Fig. 12a, the Inverse Dynamics (ID) control system is shown tracking a

Fig. 12. Position tracking performance of the BlueROV Heavy. From top to bottom: Inverse Dynamics (a), Sliding Mode (b), and Optimized Sliding Mode (c).

desired path. The ROV follows the trajectory but exhibits significant error in the z direction and some stabilization oscillations. In Fig. 12b, the Sliding Mode (SM) control system is illustrated, which provides robust position tracking and handles nonlinearities and uncertainties better than the ID control system. Lastly, Fig. 12c depicts the Optimized Sliding Mode (QP) control system, which enhances tracking performance by optimizing control inputs for greater accuracy and efficiency.

II   Effect from Disturbances

In real-world underwater environments, disturbances such as water currents and external forces are unavoidable. It is essential to assess the control system's ability to handle these disturbances.

Fig. 13 illustrates how control systems perform when exposed to disturbances (e_{dist}) compared to perfect conditions (e). The ID control system maintains stability but exhibits larger deviations under significant disturbances. The SM control system demonstrates enhanced robustness, reducing the impact of disturbances. The QP control system delivers the best performance, effectively mitigating the effects of disturbances and maintaining trajectory accuracy.
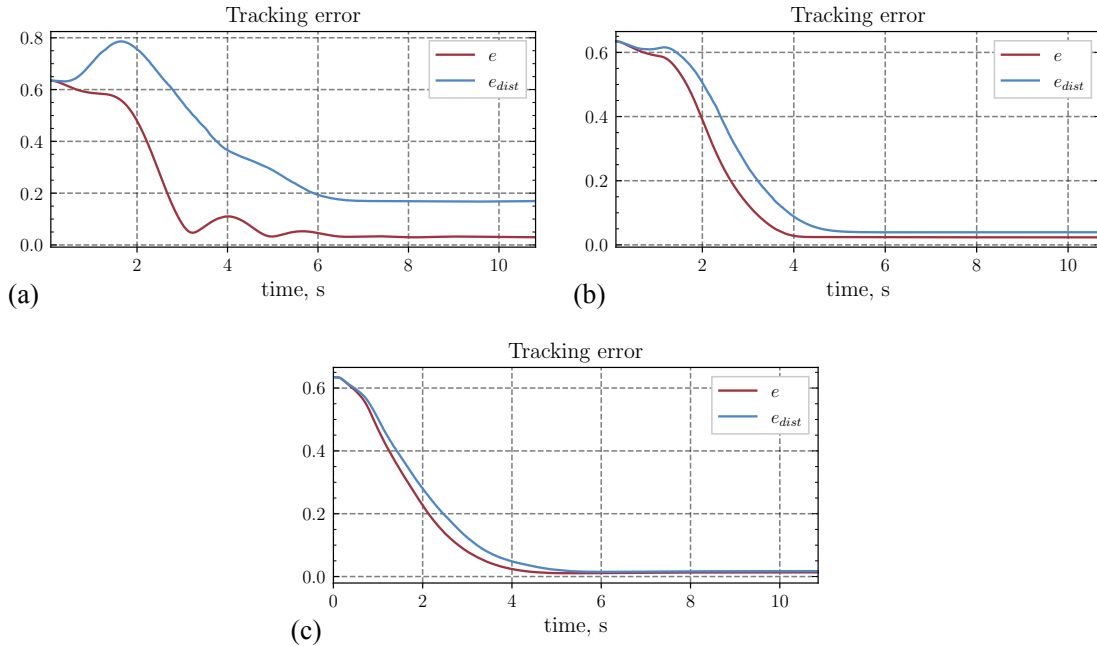
Fig. 13.   Performance of the control systems with disturbances (e_{dist}): Inverse Dynamics (a), Sliding Mode (b), and Optimized Sliding Mode (c).

III   Comparison between Control Methods

A comprehensive comparison of control methods is essential to understand their relative strengths and weaknesses, especially in terms of accuracy and energy consumption.
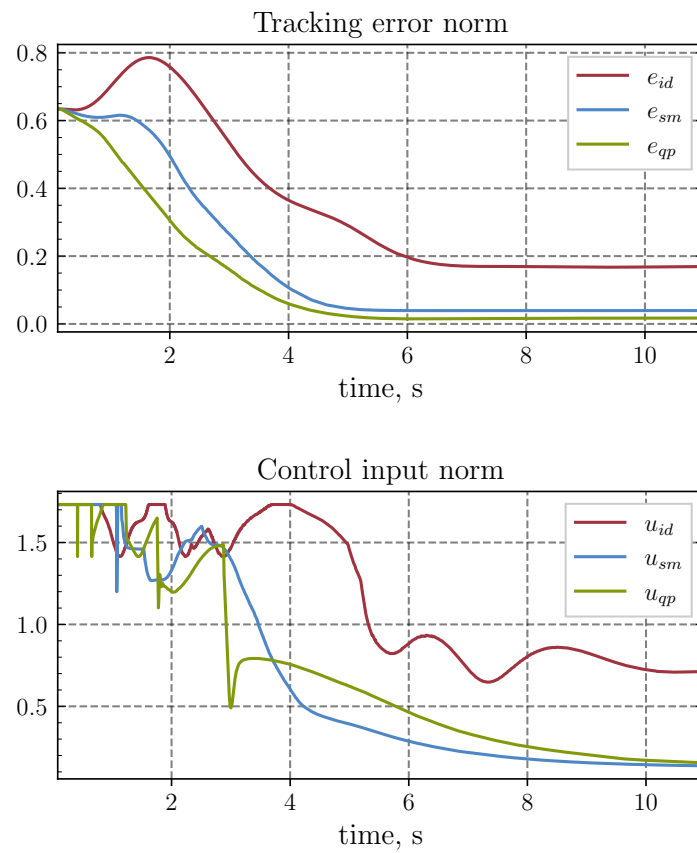

Fig. 14. Tracking error and energy efficiency metrics of the control systems: Inverse Dynamics (id), Sliding Mode (sm), and Optimized Sliding Mode (qp)

The accuracy:

- **Inverse Dynamics (ID):** Offers good accuracy under ideal conditions but is more susceptible to disturbances and modeling inaccuracies.

- **Sliding Mode (SM):** Provides better accuracy in the presence of uncertainties and disturbances due to its robust nature.

- **Optimized Sliding Mode (QP):** Delivers the highest accuracy by optimizing control inputs and effectively handling disturbances and nonlinearities.

The energy consumption:

- **Inverse Dynamics (ID):** Tends to consume more energy due to its reliance on precise model parameters and less efficient handling of disturbances.

- **Sliding Mode (SM):** Improves energy efficiency by adapting to changing conditions.

- **Optimized Sliding Mode (QP):** Optimizes thruster usage to achieve the best energy efficiency while maintaining high accuracy and robustness.

IV   Summary

After evaluating the proposed control schemes for the BlueROV Heavy in terms of position tracking, the effect of disturbances, and comparison of control methods, it is evident that the Optimized Sliding Mode (QP) control system offers the best overall performance. It effectively balances accuracy, robustness, and energy efficiency.

Chapter 7

Conclusion

This thesis addresses the challenge of controlling Remotely Operated Vehicles (ROVs) in underwater environments with nonlinearities and uncertainties. It focuses on enhancing Sliding Mode Control (SMC) using convex optimization techniques to improve stability, performance, and reduce the chattering effect.

The research's key contributions include developing a comprehensive mathematical model of an ROV and creating an advanced SMC scheme integrating convex optimization. The proposed control scheme was validated through simulations, showing improved trajectory tracking and disturbance rejection compared to traditional methods.

The findings highlight the improved stability and performance of the enhanced SMC scheme, providing better reliability and efficiency in the ROV's operation. The reduction of chattering was achieved using convex optimization, enhancing control performance and reducing wear and tear on the ROV's components.

Areas for further investigation include enhancing the computational efficiency of the convex optimization process and testing the proposed control strat-

egy in diverse underwater environments. Additionally, future research could explore integrating advanced sensing technologies to enhance the adaptability and intelligence of ROV control systems.

In summary, this thesis significantly contributes to the field of underwater robotics by providing a robust and efficient control strategy for ROVs. The integration of convex optimization with sliding mode control offers a solution that balances performance, stability, and robustness, supporting the development of more capable and reliable underwater robotic systems in challenging environments.

Bibliography cited

[1]   Y. He, D. Wang, and Z. Ali, "A review of different designs and control models of remotely operated underwater vehicle," *Measurement and Control*, vol. 53, pp. 1561–1570, Sep. 2020. DOI: 10.1177/0020294020952483.

[2]   F. Abdul Azis, M. S. Mohd Aras, M. Rashid, M. N. Othman, and S. Abdullah, "Problem identification for underwater remotely operated vehicle (rov): A case study," *Procedia Engineering*, vol. 41, pp. 554–560, Dec. 2012. DOI: 10.1016/j.proeng.2012.07.211.

[3]   L. Gutierrez, C. Zuluaga, R. Vasquez, D. Florez, E. Taborda, and R. Valencia, "Development of an underwater remotely operated vehicle (rov) for surveillance and inspection of port facilities," vol. 11, Jan. 2010. DOI: 10.1115/IMECE2010-38217.

[4]   L. Govinda, S. Tomas, M. Bandala, L. Nava Balanzar, R. Hernandez-Alvarado, and J. Antonio, "Modelling, design and robust control of a remotely operated underwater vehicle," *International Journal of Advanced Robotic Systems*, vol. 11, p. 1, Jan. 2014. DOI: 10.5772/56810.

[5]   T. Fossen, *Guidance and Control of Ocean Vehicles*. New York, NY: Wiley, 1995.

[6] B. T. Lopez and J.-J. E. Slotine, "Sliding on manifolds: Geometric attitude control with quaternions," in *2021 IEEE International Conference on Robotics and Automation (ICRA)*, 2021, pp. 11 140–11 146. DOI: 10.1109/ICRA48506.2021.9561867.

[7] S. Traversaro, S. Brossette, A. Escande, and F. Nori, "Identification of fully physical consistent inertial parameters using optimization on manifolds," in *2016 IEEE/RSJ International Conference on Intelligent Robots and Systems (IROS)*, 2016, pp. 5446–5451. DOI: 10.1109/IROS.2016.7759801.

[8] M. von Benzon, F. F. Sшrensen, E. Uth, J. Jouffroy, J. Liniger, and S. Pedersen, "An open-source benchmark simulator: Control of a bluerov2 underwater robot," *Journal of Marine Science and Engineering*, vol. 10, p. 1898, Dec. 2022. DOI: 10.3390/jmse10121898.

[9] D. Smallwood and L. Whitcomb, "Model-based dynamic positioning of underwater robotic vehicles: Theory and experiment," *IEEE Journal of Oceanic Engineering*, vol. 29, no. 1, pp. 169–186, 2004, ISSN: 0364-9059. DOI: 10.1109/joe.2003.823312.

[10] M. Spong, S. Hutchinson, and M. Vidyasagar, *Robot Modeling and Control*. Wiley, 2005, ISBN: 9780471649908.

[11] V. I. Utkin, "Variable structure systems with sliding modes," *IEEE Transactions on Automatic Control*, vol. 22, no. 2, pp. 212–222, 1977. DOI: 10.1109/TAC.1977.1101446.

[12] D. Yoerger and J. Slotine, "Robust trajectory control of underwater vehicles," *IEEE Journal of Oceanic Engineering*, vol. 10, no. 4, pp. 462–470, Oct. 1985. DOI: 10.1109/JOE.1985.1145131.

[13]   M. Spong, "On the robust control of robot manipulators," *IEEE Transactions on Automatic Control*, vol. 37, no. 11, pp. 1782–1786, 1992. DOI: 10.1109/9.173151.

[14]   V. Utkin and H.-C. Chang, "Sliding mode control on electro-mechanical systems," *Mathematical Problems in Engineering*, vol. 8, Sep. 2002. DOI: 10.1080/10241230306724.

[15]   V. I. Utkin, *Sliding Modes in Control and Optimization*. Springer Berlin Heidelberg, 1992, ISBN: 9783642843792. DOI: 10.1007/978-3-642-84379-2.

[16]   Q. Li, Y. Cao, B. Li, D. Ingram, and A. Kiprakis, "Numerical modelling and experimental testing of the hydrodynamic characteristics for an open-frame remotely operated vehicle," *Journal of Marine Science and Engineering*, vol. 8, p. 688, 2020. DOI: 10.3390/jmse8090688.

[17]   "The buoyant force and stability of floating vessels." (2024), [Online]. Available: https://www.jove.com/v/10374/the-buoyant-force-and-stability-of-floating-vessels.

[18]   Y.-Y. Chen, C.-Y. Lee, Y.-X. Huang, and T.-T. Yu, "Control allocation design for torpedo-like underwater vehicles with multiple actuators," *Actuators*, vol. 11, p. 104, Mar. 2022. DOI: 10.3390/act11040104.

[19]   J. Slotine and W. Li, *Applied Nonlinear Control* (Prentice-Hall International Editions). Prentice-Hall, 1991, ISBN: 9780130400499.

[20]   A. U. Rahman, I. Ahmad, and A. S. Malik, "Variable structure-based control of fuel cell-supercapacitor-battery based hybrid electric vehicle," *Journal*

of Energy Storage, vol. 29, p. 101 365, 2020, ISSN: 2352-152X. DOI: https://doi.org/10.1016/j.est.2020.101365.

[21] A. Rehman, M. Ashraf, and A. Bhatti, "Fixed frequency sliding mode control of power converters for improved dynamic response in dc microgrids," *Energies*, vol. 11, p. 2799, Oct. 2018. DOI: 10.3390/en11102799.

[22] H. Ozbay, A. Karafil, and S. Oncu, "Sliding mode pll-pdm controller for induction heating system," *Turkish Journal of Electrical Engineering and Computer Sciences*, vol. 29, pp. 1241–1258, Jan. 2021. DOI: 10.3906/elk-1908-62.

[23] "Bluerov2 heavy configuration retrofit kit." (2024), [Online]. Available: https://bluerobotics.com/store/rov/bluerov2-upgrade-kits/brov2-heavy-retrofit/.